Far-infrared nonlinear optics. II. $\chi^{(3)}$ contributions from the dynamics of free carriers in semiconductors

A. Mayer* and F. Keilmann
Max-Planck-Institut für Festkörperforschung, 7000 Stuttgart 80, Federal Republic of Germany
(Received 12 November 1985)

We report the first bulk frequency tripling in the far-infrared. The experiments are carried out at 20 cm^{-1} in the doped semiconductors Ge, Si, and GaAs. Good power conversion efficiency is obtained (10^{-3}). Our arrangement allows an absolute determination of the nonlinear susceptibility $\chi^{(3)}(3\omega,\omega,\omega,\omega)$. We show that in the far-infrared, $\chi^{(3)}$ is dominated by free-carrier contributions. Hence, our measurement gives new insight into nonlinear transport properties such as the momentum dependence of the effective mass and of the relaxation time. Furthermore strong changes of $\chi^{(3)}$ (as well as of the absorption) are found to occur at high laser intensity above 100 kW/cm^2, which we attribute to carrier heating and hot carrier transfer into higher energy-band minima.

I. INTRODUCTION

Nonlinear optical work has only recently been extended into the far-infrared spectral range. In this development, the important steps were the achievement of both high-contrast spectral filters and of absolute intensity calibration. These techniques are described in Sec. II of the preceding paper[1] (designated as I hereafter) and will not be repeated here.

Nonlinear optical effects due to free carriers in semiconductors were first studied[2-6] in the microwave region, where they arise from the nonlinear relation between drift velocity and applied electric field. Some years later, nonlinear optics studies were carried out at mid-infrared frequencies, when Patel *et al.* observed frequency mixing of CO_2 laser beams due to free carriers in III-V compounds.[7] Wolff and Pearson explained the results by anharmonic motion of carriers in nonparabolic bands.[8] Distinct from this, a second possible mechanism arises from the nonlinearity associated with a dependence of the carrier relaxation time on momentum. While both mechanisms can yield comparable nonlinearity, the latter has not been observed in an experiment before.

Both mechanisms are expected to be strongly frequency dependent: Relaxation denominators increase the calculated nonlinear susceptibilities as the frequency ω decreases. This behavior comes to an end when $\omega\tau\approx 1$, where τ is the carrier relaxation time. Such a frequency dependence was recently observed[9] by tuning the difference frequency $\omega_2-\omega_1$ of two CO_2 laser beams in a four-wave mixing experiment, in which a beam at $\omega_3=2\omega_2-\omega_1$ was generated.

In the present work, the free-carrier nonlinearity is measured at infrared frequencies below that of the CO_2 laser for the first time. The low-frequency regime offers distinct advantages. First, the discrimination from the bound-electron contribution to the nonlinear susceptibility becomes very easy since the latter is independent of frequency and in fact dominates at CO_2 laser frequency. At low frequency, the free-carrier contribution can thus be obtained in the interesting regime of very low carrier concentration. A second advantage of a far-infrared measurement is the fact that multiphoton interband effects play no role even in narrow-gap semiconductors. Finally, it is in the far infrared where an interesting transition can be expected to occur: from a single-carrier nonlinearity at high frequency, to the drift-velocity-based nonlinearity measured at microwave frequency.

All this makes the far-infrared studies of nonlinear susceptibility an attractive tool to test theoretical concepts of carrier dynamics and of band structure. In Sec. II we describe our experimental procedure to determine $\chi^{(3)}$ by frequency tripling. Section III gives the existing transport-theoretical description of free-carrier nonlinear susceptibility. In Sec. IV we present our results and discuss the nonlinear susceptibility and band-structure data which we obtained. We further discuss an observed decrease of $\chi^{(3)}$ at high laser intensity by considering carrier heating.

II. EXPERIMENTAL METHOD

We determine the nonlinear susceptibility $\chi^{(3)}$ by bulk frequency tripling of short laser pulses. Both setup and procedure are analogous to those used for frequency doubling as described in I.[1] The equation which relates $\chi^{(3)}$ to measured quantities is Eq. (5) of I, with $n=3$,

$$L_{3\omega}(t)=\left[\frac{128\pi^2}{c}\right]^2\left|\frac{N_{3\omega}+1}{(N_\omega+1)^2}\right|^2|\chi^{(3)}|^2[L_\omega(t)]^3 \times\frac{8}{\pi w^2}\int|C(d)|^2\exp(-6r^2/w^2)dF\,, \quad (1)$$

where L_ω is the incident fundamental power, $L_{3\omega}$ is the resulting third harmonic power. A near-fundamental Gaussian mode profile $E\sim\exp(-r^2/w^2)$ is assumed where w is the spot radius. N is the complex refractive index defining the coherence factor C [see Eq. (2) in I], d is the sample length. In the experiment, we detect the

harmonic pulse energy

$$W_{3\omega}=\int L_{3\omega}(t)dt\sim\int[L_{\omega}(t)]^3dt\ . \tag{2}$$

The latter integral is obtained numerically using the time-resolved fundamental signal $L_{\omega}(t)$.

There are no problems in separating second-harmonic radiation, which is simultaneously generated in noncentrosymmetric crystals such as GaAs, by standard filters.

The samples were in the form of single crystals with polished surfaces. Wedge shapes were used to allow a continuous change of the sample length d. Optically thin samples were usually used to facilitate corrections for absorption. For samples with high carrier concentration (10^{15} cm^{-3}) this necessitated thicknesses of only a few μm, achieved in the case of GaAs by epitaxial growth on semi-insulating wedge-shaped substrates. As an example of the measurements, Fig. 1 shows the measured third-harmonic pulse energy as a function of crystal length for n-Si. The data are fit to Eq. (1) with $\chi^{(3)}$ as the only fitting parameter. This procedure of obtaining $\chi^{(3)}$ requires accurate knowledge of the complex refractive indices. However, since Maker fringes are not visible in Fig. 1, any possible dispersive effects are greatly dominated by absorption, and phase matching presents no problem. Note that absorption is due to the free carriers. The absorption both of the fundamental and harmonic waves was measured accurately. We used similar procedures as described in Appendix A of I. The refractive indices were calculated by taking into account the optical properties of the free carriers in a Drude model. Details characterizing the samples used may be found in the thesis Ref. 4 in I.

In the cubic crystal investigated the tensor $\chi^{(3)}(3\omega,\omega,\omega,\omega)$ has two independent components (Ref. 11), $\chi^{(3)}_{1111}$ and $\chi^{(3)}_{1122}$. For the orientation shown in the insert of Fig. 1, $\chi^{(3)}_{\rm eff}=\chi^{(3)}_{1111}$. If the crystal is rotated around the propagation direction by 45°, the input (and output) field is polarized along a [110] direction. In this case, the measured nonlinear susceptibility is $\chi^{(3)}_{\rm eff}=\frac{1}{2}(\chi^{(3)}_{1111}+3\chi_{1122})$. The anisotropy of $\chi^{(3)}$ can thus be expressed by the ratio of the $\chi^{(3)}_{\rm eff}$'s in both orientations, $\sigma=\frac{1}{2}+\frac{3}{2}(\chi_{1122}/\chi_{1111})$. An example of the measurement is shown in Fig. 2.

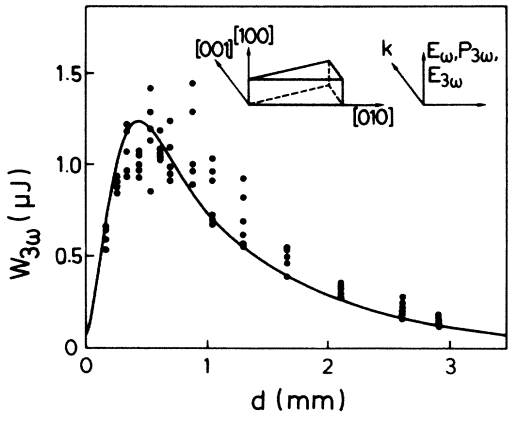

FIG. 1. Third-harmonic pulse energy produced in n-Si with a free-electron concentration $n_e=2.7\times10^{15}$ cm^{-3} at room temperature, versus crystal length d. The input pulse energy is 1.1 mJ, at the fundamental frequency of 20.2 cm^{-1}. The solid line is a fit to Eq. (1). The inset shows the orientation of the sample crystal, cut as a wedge with an apex angle of 5°. The polarizations of fundamental and harmonic fields are also indicated.

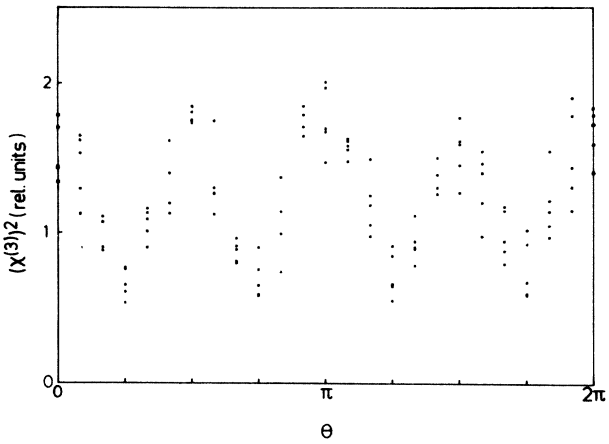

FIG. 2. Measured square of third-order susceptibility $\chi^{(3)}_{\rm eff}$ of p-Si ($n_h=4.5\times10^{16}$ cm^{-3}) versus orientation angle θ, at room temperature. The sample is a 278-μm-thick plate with (100) surfaces. Linearly polarized 20.2 cm^{-1} radiation enters at normal incidence. θ measures rotation of the plate around an axis parallel to the beam direction. $\theta=n\pi/2$, $n=0,1,\ldots$ occurs when the polarization is parallel to a [110] direction. From the ratio of maximum to minimum we can read out the anisotropy $\sigma=(2.1\pm0.2)^{1/2}$ (see text).

III. THEORY

In semiconductors, the third-order nonlinear susceptibility $\chi^{(3)}$ arises from the lattice, the bound electrons, and the free electrons. The former two contributions being small,[1,10,12] we deal here only with the latter.

Free-electron nonlinearity was first studied in the microwave region,[2–6] where $\omega\tau\ll1$. Here the carrier temperature can adiabatically follow the oscillating electric field, and thus a modulation of the drift velocity results.

In the infrared where $\omega\tau\gg1$ holds we can describe the individual carrier motion in a simple oscillator picture

$$m(v)\dot{v}+\frac{m(v)v}{\tau(v)}=eE_0\cos(\omega t)\ , \tag{3}$$

where E_0 is the amplitude of the field, and e, m, v, and τ denote charge, mass, velocity, and relaxation time of the carrier. This formulation assumes two distinct nonlinear processes, the band nonparabolicity described by $m(v)$ and the dependence of the relaxation time on the velocity $\tau(v)$. Clearly, a solution of Eq. (3) contains harmonic components of the motion, which give rise to harmonic radiation.

The full Boltzmann's equation treatment of the problem has been given by Wang and Ressler[13] and Rustagi.[14] They considered the momentum and time distribution $f(p,t)=f_0+f_1+\cdots$ of the free carriers, in the presence of radiation at frequency ω. We assume a single band and

quote the result[13] for the frequency-tripling nonlinear susceptibility

$$\chi^{(3)}=2\frac{-5}{(3)36\pi^2}\frac{e^4}{\hbar^3}\int_0^\infty f'_0\beta_2 p^3(x+y+z)dp^2 , \quad (4)$$

where the leading factor of 2 has been added because of our definition of $\chi^{(3)}$ (Sec. II in I), and $\beta_2=3/[2\omega(i\omega+1/\tau)]$. In the integral of Eq. (4), x describes the nonparabolicity and y the relaxation contributions, while z is a mixed term, important only when both contributions are of similar magnitude,

$$x=g(1+\tfrac{4}{5}\beta_1)(I'+\tfrac{2}{5}p^2I'') , \quad (5)$$

$$y=I(\tfrac{8}{25}p^2\beta'_1g'_1+(1+\tfrac{4}{5}\beta_1)(g'+\tfrac{2}{5}p^2g'')] , \quad (6)$$

$$z=\tfrac{8}{25}p^2I'[\beta'_1g+(2\beta_1+\tfrac{5}{2})g'] , \quad (7)$$

where $\beta_1=2i\omega/(2i\omega+1/\tau)$, $g=1/(3i\omega+1/\tau)$, and $I=1/m^*(p)$ with m^* the effective mass. Wang and Ressler[13] have calculated the integral for a dominant nonparabolicity contribution, $x\gg y,z$, in the limit $\omega\tau\gg1$. In our case of far-infrared frequencies, $\omega\tau\gtrsim1$, we can obtain an analytic integral for the nonparabolicity term x, if we assume τ independent of p. The integral for the relaxation term y has to be evaluated numerically. We now consider three cases.

A. *n* type, direct gap: GaAs

We calculate the nonparabolicity contribution by using Kane's model of the band structure

$$W(k)=\frac{E_g}{2}\left[\left[1+\frac{2\hbar^2k^2}{m_0^*E_g}\right]^{1/2}-1\right] , \quad (8)$$

where W and k denote energy and wave vector of the electrons, E_g is the energy gap, and m_0^* the effective mass at the band edge,

$$m^*(k)=m_0^*\left[1+\frac{2\hbar^2k^2}{m_0^*E_g}\right]^{1/2} . \quad (9)$$

Assuming $\tau(p)=\text{const}=m_0^*\mu/e$, where μ is the mobility, we obtain the nonlinear susceptibility from Eqs. (4) and (5),

$$\chi^{(3)}=\frac{-10i}{36\omega}\frac{1}{(1/\tau)+i\omega}\frac{1}{(1/\tau)+3i\omega}\left[\frac{1}{2i\omega}+\frac{4}{5}\frac{1}{(1/\tau)+2i\omega}\right]\frac{n_ee^4}{(m_0^*)^2E_g}\left[1+\frac{6k_BT}{E_g}\right]^{-7/2} , \quad (10)$$

where T and k_B denote the temperature and Boltzmann's constant of the assumed nondegenerate electron distribution.

The relaxation contribution unfortunately cannot be calculated. The reason is that the models available cannot treat the case of polar optical scattering which however is dominant in room-temperature GaAs.

B. *n* type, indirect gap: Si,Ge

First, we discuss the nonparabolicity contribution. The energy surfaces near the conduction-band minima are ellipsoids,

$$W(k)=\frac{n^2k_\perp^2}{2m_\perp}+\frac{n^2k_\parallel^2}{2m_\parallel}+\eta_1k_\perp^4+\eta_2k_\parallel^2k_\perp^2+\eta_3k_\parallel^4 . \quad (11)$$

The anisotropy of the band structure leads to an anisotropy of the nonlinear polarization.[15,16] If ψ denotes the angle between electric field and long axis of an ellipsoid, the nonlinear polarization becomes

$$P_\parallel^{(3)}\sim\eta_3\cos^3\psi+\frac{\eta_2}{2}\sin^2\psi\cos\psi ,$$
$$P_\perp^{(3)}\sim\eta_1\sin^3\psi+\frac{\eta_2}{2}\sin\psi\cos^2\psi . \quad (12)$$

To obtain $\chi^{(3)}$ we have to average, in the case of Si, over six ellipses oriented in the [100] direction. For the special case of E parallel to [100] we obtain

$$\chi^{(3)}_{1111}(3\omega,\omega,\omega,\omega)=(\tfrac{6}{4}\eta_1+\tfrac{2}{6}\eta_3)\frac{-4n_ee^4}{g\hbar^4\omega^2}\frac{1}{(1/\tau)+i\omega}\times\left[\frac{5}{4}+\frac{2i\omega}{(1/\tau)+2i\omega}\right]\frac{1}{(1/\tau)+3i\omega} \quad (13)$$

The band-structure coefficients can be obtained from kp perturbation[18] to be

$$\eta_1=-\hbar^4/(4m_\perp^2E_{\text{dir}}) \quad (14)$$

and $\eta_3\ll\eta_1$, where E_{dir} is the direct gap energy. For Ge, the band-structure coefficients have been calculated taking into account the interaction of the conduction band with several other bands:[16]

$$\eta_1=1.4\hbar^4/(4m_\perp^2E_{\text{dir}})(1-m_\perp/m_e)^2 ,$$
$$\eta_2=0.5\eta_1,\quad \eta_3=0.0036\eta_1 .$$

Using the result of Cardona and Pollack quoted in Ref. 14 for the average over the four tetrahedrally oriented conduction-band minima we obtain

$$\chi^{(3)}_{1111}=-0.8\frac{n_ee^4\eta_1}{\hbar^4\omega^2}\frac{1}{(1/\tau)+i\omega}\times\left[\frac{5}{4}+\frac{2i\omega}{(1/\tau)+2i\omega}\right]\frac{1}{(1/\tau)+3i\omega} . \quad (15)$$

Next, we consider the relaxation contribution to the third-order nonlinear susceptibility, to be calculated by

numerical integration of y [Eqs. (4) and (6)]. For Si and Ge, this requires that we approximate the anisotropic band structure by an angular average. The total relaxation rate is, for room temperature and densities $10^{13} < n_e < 10^{17}$ cm^{-3}, the sum of two contributions, $\tau^{-1} = \tau_a^{-1} + \tau_i^{-1}$, where $\tau_a^{-1} \sim p$ is the rate of acoustic phonon scattering which is known from mobility measurements at low doping, and $\tau_i^{-1} \sim p^{-3}$ results from treating ionized impurity scattering by the Brooks-Herring formula.[19]

C. p-type semiconductors

No explicit theories have yet been formulated for the third-order nonlinearity of the valence bands. The reason for this may be the higher complexity of the band structure and also differences in relaxation rates between the different valence bands. Thus, our experimental results on $\chi^{(3)}$ cannot yet be linked to nonparabolicity and relaxational contributions.

A paper by Lax *et al.*[17] is noteworthy; it predicts that frequency tripling of circularly polarized light occurs through the warping of valence bands.

IV. RESULTS AND DISCUSSION

In Fig. 3 the data points show our experimental values of $\chi^{(3)}$ in n-type semiconductors. The error bars are mainly due to the uncertainty of absolute intensity calibration. Within the error bars, the nonlinear susceptibility is proportional to the carrier density, and thus represents a single-carrier effect.

The theoretical curves in Fig. 3 are calculated from Eq. (4). First we consider n-Si. The nonparabolicity contribution (solid curve) was obtained by using, in Eq. (13), the value $\eta_1 = -1.5 \times 10^{-42}$ erg cm^4 from kp perturbation. The relaxation contribution (dashed curve) results from Eqs. (6) and (4). Both curves show saturation at high carrier density, due to increased ionized impurity scattering.

Both contributions come out nearly equal. Note that both contributions have nearly the same phase and therefore add. Evaluation of the mixed term Eq. (7) shows it is negligibly small. The sum of both theoretical contributions seems to just match the observed data. However, the nonparabolicity contribution becomes larger when we use higher values of η_1, as they come out from two experimental studies: Cyclotron resonance measurements[20] yield $\eta_1 = -(6.4 \pm 3.2) \times 10^{-42}$ erg cm^4, while the infrared Faraday effect[21] results in even $|\eta_1| = 16 \times 10^{-42}$ erg cm^4. With these numbers, the nonparabolicity effect alone could account for the data.

We have furthermore measured the anisotropy (Sec. II) of $\chi^{(3)}$. For n-Si with $n_e = 2.7 \times 10^{15}$ cm^{-3}, we obtain $\sigma = 0.86 \pm 0.02$.

We turn now to n-Ge (Fig. 3). The nonparabolicity contribution is calculated by using $\eta_1 = -1.8 \times 10^{-41}$ erg cm^4 from kp perturbation. A full match of the nonparabolicity contribution to the experimental data would require $|\eta_1| = 3.4 \times 10^{-41}$ erg cm^4. Other determinations of η_1 are in overall agreement, as magnetopiezo experiments[22] have yielded $\eta_1 = -2.5 \times 10^{-41}$ erg cm^4, and cyclotron resonance experiments have given $\eta_1 = -(4 \pm 2) \times 10^{-41}$ erg cm^4 (Ref. 20) and $\eta_1 = -2.0 \times 10^{-41}$ erg cm^4 (Ref. 23). The relaxation contribution is distinctly smaller (Fig. 3). We conclude that we have good agreement between theory and experiment.

Next we plot, for n-Ge, the theoretical nonparabolicity contribution [Eq. (15)] to $\chi^{(3)}$ as a function of frequency (Fig. 4). We note an ω^{-4} dependence in the infrared. The agreement with a previous determination using a CO_2 laser[16] is good. Figure 4 shows that in the near infrared the free-carrier effects can hardly be seen on the background of the bound-carrier contribution, except at very high carrier concentration. No such problem exists in the far infrared.

Our measurements on n-Ge, at $\omega = 20.2$ cm^{-1}, further yields an anisotropy $\sigma = 1.16 \pm 0.05$, using a sample with $n_e = 1.2 \times 10^{15}$ cm^{-3}. This agrees with the values given by Wang and Ressler[16] who found $\sigma = 1.18$ from theory and $\sigma = 1.20$ from the experiment. We finally note that a more accurate determination of σ could be obtained by applying uniaxial pressure which would transfer all free carriers to a single conduction-band minimum.

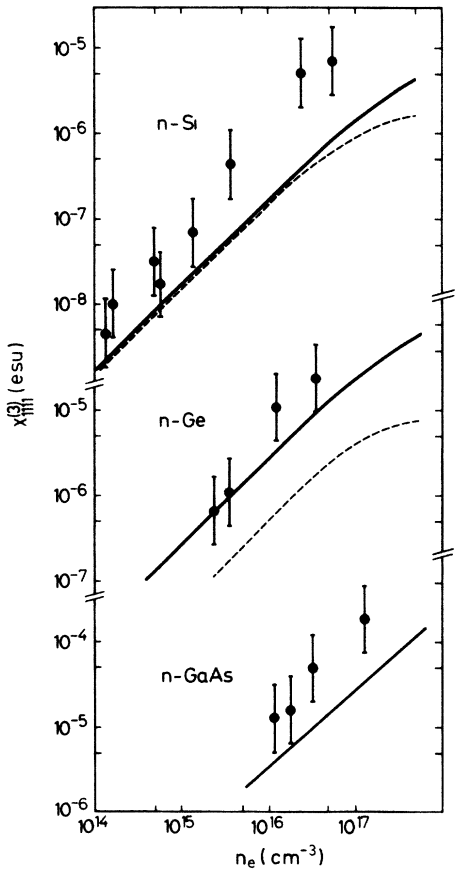

FIG. 3. Absolute values of third-order nonlinear susceptibility $\chi^{(3)}_{1111}(3\omega,\omega,\omega,\omega)$ measured by frequency tripling of 20.2 cm^{-1} radiation, versus free-electron concentration, for n-type Si, Ge, and GaAs at room temperature. The curves are theoretical predictions for the nonparabolicity (solid) and relaxation (dashed) contributions, respectively.

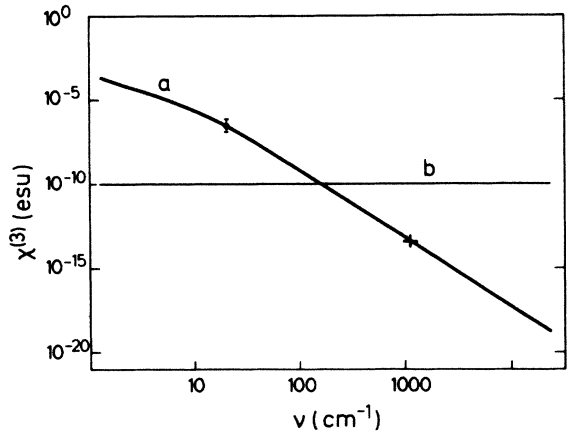

FIG. 4. Absolute value of third-order nonlinear susceptibility $\chi^{(3)}_{1111}(3\omega,\omega,\omega,\omega)$ of room temperature n-Ge with $n_e=10^{14}$ cm^{-3}. a, theoretical curve based on band nonparabolicity [Eq. (15)]. b, contribution of bound electrons (Ref. 10). The data point at 20.2 cm^{-1} is from this work; the cross near 1000 cm^{-1} represents the linear extrapolation of a measurement by Wang and Ressler (Ref. 16), where a sample with $n_e=2.1\times10^{17}$ was used.

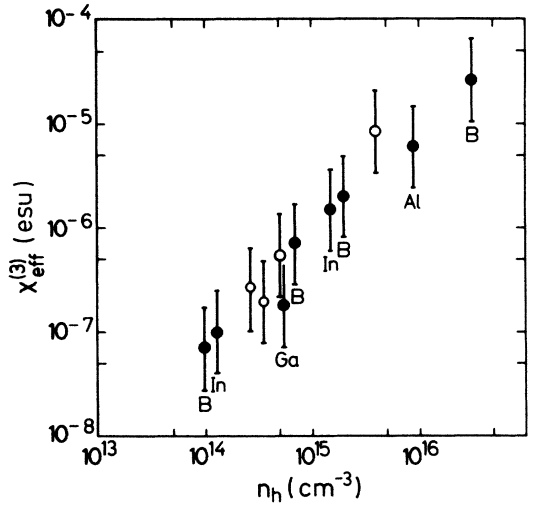

FIG. 5. Absolute values of third-order nonlinear susceptibility $\chi^{(3)}_{eff}(3\omega,\omega,\omega,\omega)$ of p-Si (filled circles) and p-Ge (open circles, In doped) measured at room temperature and $\nu=20.2$ cm^{-1}. For Ge crystals the orientation was such that $\chi^{(3)}_{eff}=\chi^{(3)}_{1111}$, while for the Si crystals $\chi^{(3)}_{eff}=\sigma\chi^{(3)}_{1111}$.

Our results for n-GaAs are shown in the bottom part of Fig. 3. No theoretical curve can be given here for the relaxation contribution. The nonparabolicity contribution [Eq. (10)], calculated with Kane's band structure, is lower than the experimental value by a factor of 3.5 ± 1.5. A similar mismatch (3 ± 1.5) was noted by Wynne[10] in a mixing experiment at 10 μm wavelength. He ascribed this to a failure of Kane's model for the case of GaAs, where higher order conduction bands ought to be included in the model. Rössler[24] has extended the model accordingly. However, his result is a correction of 8% only in the k^4 term relevant to us here, and thus cannot explain the discrepancy.

The anisotropy of GaAs was measured to be $\sigma=1.11\pm0.02$, in a sample with $n_e=1.3\times10^{16}$ cm^{-3} at $\nu=45$ cm^{-1}. In contrast the experiments of Wynne[10] gave no anisotropy. If we write the the fourth-order term of the band structure [Eq. (8)] in the form

$$\alpha k^4+\beta(k_y^2k_z^2+k_x^2k_z^2+k_x^2k_y^2)\ ,$$

we have $\sigma=1+\beta/4\alpha$. Inserting Kane's parameters, we obtain $\sigma=1.17$, while after Rössler[24] we expect, at room temperature, $\sigma=1.29$. The experimental anisotropy is thus smaller than predicted for the nonparabolicity contribution. This may point to an influence of relaxation (qualitatively we note the strong dependence of τ on p near room temperature).[25] If we assume a relatively strong relaxation contribution, viz., 2.5:1, to make up for the discrepancy in Fig. 3, we accordingly have to reduce the anisotropy from 1.29 to $(1.29\pm2.5)/3.5=1.08$. This value is in near agreement with the experimental result.

Our results on p-type Si and Ge are summarized in Fig. 5. Within the error bars, the nonlinear susceptibility is proportional to the hole density, and independent of the nature of the acceptor. In addition, the anisotropy is mea-

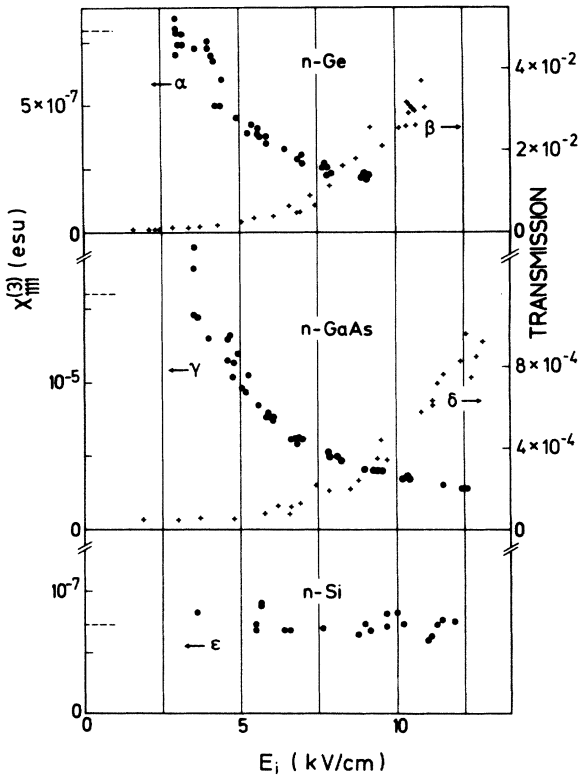

FIG. 6. Experimental results of high-intensity bleaching of both the absorption and the nonlinear susceptibility of room temperature n-Ge (α,β) and n-GaAs (γ,δ). The effect is absent in n-Si (ϵ). The frequency is 20.2 cm^{-1}. The abscissa E_i is the incident fundamental electric field amplitude just inside the crystal. The value of $\chi^{(3)}$ at low intensity is marked with a dashed line. The sample characteristics are as follows, in a sequence chemical identity, carrier concentration, and thickness. α: Ge, 2.5×10^{14} cm^{-3}, 1.68 mm. β: Ge, 1.3×10^{15} cm^{-3}, 1.73 mm. γ: GaAs, 2.1×10^{15} cm^{-3}, 33 μm. δ: GaAs, 2.1×10^{16} cm^{-3}, 94 μm. ϵ: Si, 1.4×10^{14} cm^{-3}, 4.2 mm.

sured for a Si:B sample with $n_h = 4.5 \times 10^{16}$ cm^{-3} to be $\sigma = 1.61 \pm 0.06$.

While the results described so far were obtained at medium laser intensity, we turn now to changes of $\chi^{(3)}$ which become observable at high intensity: The nonlinearity decreases, and at the same time the absorption is also seen to decrease. The results for three semiconductors are shown in Fig. 6. [Although $\chi^{(3)}$ now depends on the intensity, we have as an approximation still used Eq. (2) in this evaluation.] Here the abscissa is the incident fundamental electric field amplitude inside the crystal, E_i at $z=0$, which is derived from our measurement of incident pulse energy (i) by dividing by 40 ns [Fig. 1(b) in I] to obtain an average peak power, (ii) by dividing by 0.063 cm^2 [Fig. 1(a) in I] to obtain an average peak intensity I, and (iii) by evaluating $E_i = [2I/\epsilon_0 nc]^{1/2}$, where ϵ_0 is the permittivity of free space, n is the refractive index, and c the speed of light. We see that in the power range accessible to us, $\chi^{(3)}$ decreases to about $\frac{1}{4}$ and $\frac{1}{5}$, respectively, for n-Ge and n-GaAs, whereas no change from the low-intensity value is found for n-Si.

We attribute this result to radiation-induced heating. An effect of heating the lattice can, however, be ruled out from a simple estimation. An absorbed pulse energy of maximum 2 mJ and a spot diameter $2w = 4$ mm gives a maximum fluence of 30 mJ/cm^2, which if absorbed in a depth of 100 μm, gives an absorbed energy density of 3 mJ/cm^3, equivalent to a heating of only 8 K (in Ge). Let us therefore examine heating of the free carriers. From Drude theory the absorption cross section of a typical free carrier is $S \lesssim 3 \times 10^{-14}$ cm^2. Assuming a strong ac electric field with an amplitude of 5 kV/cm, corresponding (in Ge) to an intensity of $I = 133$ kW/cm^2, we obtain the absorbed power per free carrier to be $SI \lesssim 25$ meV/ps. Since this value is in the order of magnitude of one optical phonon energy per collisional lifetime, we can expect hot-electron effects.

We believe that our observations of saturated far-infrared absorption, as well as of saturated nonlinearity of free carriers, are both due to a radiation-induced perturbation of the carrier distribution in ω-k space. The states gaining population thus must have the twofold property of (i) a reduced absorption of the radiation and (ii) a reduced nonlinear susceptibility. Three classes of states can be discussed. First let us consider heating within the lowest conduction band. In this case we expect an increase of the absorption because the mass decreases with energy while the scattering rate increases ($\omega\tau \approx 1$ at low intensity). Since we observe, on the contrary, a decrease of the absorption, we can rule out simple heating within the band. A second possibility for n-Ge is a population transfer into equivalent valleys. Depending on its orientation in the electric field, a valley can become more or less strongly heated. As a consequence, intervalley transfer occurs from hot to colder valleys. However, this effect must disappear when the electric field is in a [100] direction. Such an anisotropy of the saturation behavior is not, however, observed.

Let us turn to the third possibility of carrier scattering into nonequivalent valleys. There are "siliconlike" valleys in Ge in [100] directions 0.18 eV above the [111] minima. GaAs has [100] valleys 0.36 eV above the $k=0$ central valley. Population transfer into these higher valleys has been studied by applying high electric fields.[26] In the case of GaAs the mobility is found to be much reduced in the upper valley (increased mass), which leads to the appearance of negative differential conductivity at dc field strengths above 3 kV/cm. In our experiment we find the nonlinear effects to occur with the far-infrared ac fields of about this magnitude. A reduced far-infrared absorption is expected from the increased mass in the upper valleys. In addition, we expect $\chi^{(3)}$ to decrease from the increase of both mass and $E_{\rm dir}$, according to Eqs. (14) and (13). Moreover, saturation effects could not be found in Si where the population of higher valleys is known to require even higher field strength. Altogether, we therefore conclude that the population transfer by strong THz fields is responsible for both observed saturation effects. On this basis it should be possible to use our data for calculating nonparabolicity and relaxation characteristics in higher valleys.

V. CONCLUSIONS

Far-infrared nonlinear spectroscopy has been introduced as a new tool to study semiconductor carrier dynamics. At medium laser intensities, efficient frequency tripling is observed. The pertaining nonlinear susceptibility $\chi^{(3)}$ which is absolutely measured agrees with model calculations based on both band nonparabolicity and on energy-dependent relaxation, for n-Ge and n-Si. No theory yet exists for p-Ge, p-Si, and n-GaAs to compare with our experimental results.

At high far-infrared intensity, we observe hot electron effects occurring. Both the absorption and the nonlinear susceptibility are found to decrease in n-Ge and n-GaAs. At the critical intensity the equivalent ac electric field amplitude is of the same order of magnitude as the critical dc electric fields where intervalley transfer and negative differential conductivity are known to occur.

ACKNOWLEDGMENTS

We would like to thank M. Cardona, W. Zawadzki, and R. Bray for helpful discussions. The supply of samples by W. Zulehner (Wacker-Chemietronic) is gratefully acknowledged.

*Present address: Prognos A6, Steinengraben 42, 4011 Basel, Switzerland.

[1] A. Mayer and F. Keilmann, preceding paper, Phys. Rev. B 33, 6954 (1986).

[2] B. V. Paranjape, Phys. Rev. 122, 1372 (1961).

[3] P. Das, Phys. Rev. 138, A590 (1965).

[4] K. Seeger, J. Appl. Phys. 34, 1608 (1963).

[5] S. Kobayashi, S. Yabuki, and M. Aoki, Jpn. J. Appl. Phys. 2,

127 (1963).
[6]G. Nimtz and K. Seeger, J. Appl. Phys. **39**, 2263 (1968).
[7]C. K. N. Patel, R. E. Slusher, and P. A. Fleury, Phys. Rev. Lett. **17**, 1011 (1966).
[8]P. A. Wolff and G. A. Pearson, Phys. Rev. Lett. **17**, 1015 (1966).
[9]S. J. Yuen and P. A. Wolff, Appl. Phys. Lett. **40**, 457 (1982).
[10]J. J. Wynne, Phys. Rev. **178**, 1295 (1969).
[11]P. D. Maker, R. W. Terhune and C. M. Savage, in *Proceedings of the Third International Conference on Quantum Electronics,* edited by P. Grivet and N. Bloembergen (Dunod, Paris, 1963), p. 1559.
[12]W. K. Burns and N. Bloembergen, Phys. Rev. B **4**, 3437 (1971).
[13]C. C. Wang and N. W. Ressler, Phys. Rev. **188**, 1291 (1969).
[14]K. C. Rustagi, Phys. Rev. B **2**, 4053 (1970).
[15]S. S. Jha and N. Bloembergen, Phys. Rev. **171**, 891 (1968).
[16]C. C. Wang and N. W. Ressler, Phys. Rev. B **2**, 1827 (1970).
[17]B. Lax, W. Zawadzki, and M. H. Weiler, Phys. Rev. Lett. **18**, 462 (1967).
[18]E. O. Kane, in *Semiconductors and Semimetals,* edited by R. K. Willardson, and A. C. Beer (Academic, New York, 1966), Vol. 1.
[19]H. Brooks, Phys. Rev. **83**, 879 (1951).
[20]J. C. Ousett, J. Leotin, S. Askenazy, M. S. Skolnick, and R. A. Stradling, J. Phys. C **9**, 2803 (1976).
[21]A. K. Walton and P. L. Reimann, J. Phys. C **3**, 1410 (1970).
[22]R. L. Aggarwal, M. T. Zuteck, and B. Lax, Phys. Rev. **180**, 800 (1969).
[23]N. Miura, G. Kido, and S. Chikazumi, Solid State Commun. **18**, 885 (1976).
[24]U. Rössler, Solid State Commun. **49**, 943 (1984).
[25]H. J. Ehrenreich, J. Appl. Phys. **32**, 2155 (1961).
[26]K. Seeger, *Semiconductor Physics,* Vol. 40 of *Springer Series in Solid-State Sciences* (Springer, Berlin, 1982).